Supplementary Information

Characterization of a selective inhibitor of the Parkinson's disease kinase LRRK2

Xianming Deng[1,6], Nicolas Dzamko[2,6], Alan Prescott[3], Paul Davies[2] ,Qingsong Liu[1], Qingkai Yang[4], Jiing-Dwan Lee[4], Matthew P. Patricelli[5], Tyzoon K. Nomanbhoy[5], Dario R. Alessi[2,*] and Nathanael S. Gray[1,*]

1. Department of Cancer Biology, Dana-Farber Cancer Institute, and Department of Biological Chemistry & Molecular Pharmacology, Harvard Medical School, 250 Longwood Ave, SGM 628, Boston, MA 02115, USA. 2. MRC Protein Phosphorylation Unit, College of Life Sciences, University of Dundee, Dow Street, Dundee DD1 5EH, Scotland. 3. Division of Cell Biology and Immunology, College of Life Sciences, University of Dundee, Dow Street, Dundee DD1 5EH, Scotland 4. Department of Immunology and Microbial Science, The Scripps Research Institute, 10550 North Torrey Pines Road, La Jolla, CA 92037, USA. 5. ActivX Biosciences, 11025 North Torrey Pines Road, La Jolla, CA 92037, USA. 6. These authors contributed equally to this work.

[*]*Corresponding author: Nathanael S. Gray, nathanael_gray@dfci.harvard.edu Tel: 1-617-582-8590, FAX: 1-617-582-8615. Dario R. Alessi, d.r.alessi@dundee.ac.uk, Tel: 44-1382-385602, FAX: 44-1382- 223778.*

Contents

Supplementary methods

1. Synthesis of LRRK2-IN-1 (1)

Scheme 1

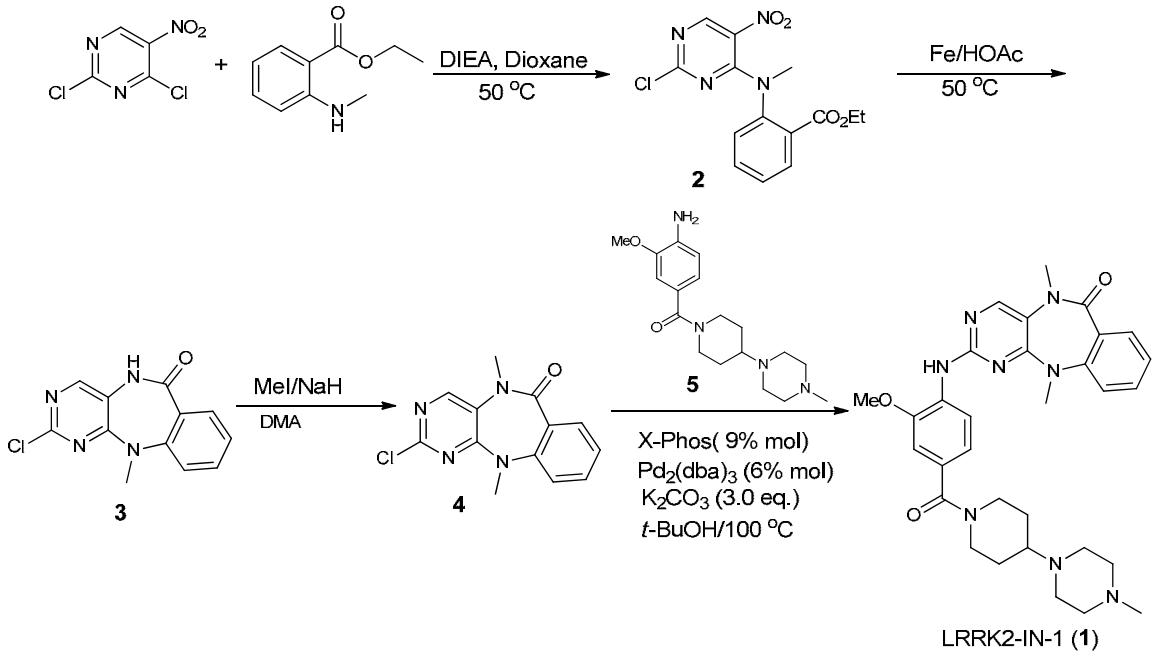

a)

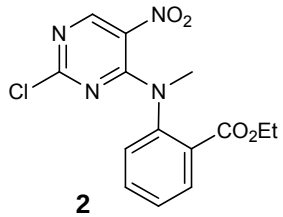

2

A mixture of ethyl 2-(methylamino)benzoate (1.44 g, 8.0 mmol), diisopropyl ethylamine (DIEA) (2.8 mL, 16.0 mmol) and 2,4-dichloro-5-nitropyrimidine (2.30 g, 12.0 mmol) in dioxane (40 mL) was heated at 50˚C for 6 hours. After the reaction was complete as monitored by thin layer chromatography (TLC), the reaction solution was concentrated and the residue was purified by silica-gel column chromatography with ethyl acetate and hexane (1/20, v/v) to give the title compound **2** (2.51 g, 93%). ^{1}H NMR (600 MHz, $CDCl_3$) δ 8.44 (s, 1H), 8.02 (d, *J* = 7.2 Hz, 1H), 7.59 (t, *J* = 7.2 Hz, 1H), 7.44 (t, *J* = 7.2 Hz, 1H), 7.22 (d, *J* = 7.8 Hz, 1H), 4.28-4.18 (m, 2H), 3.58 (s, 3H), 1.29 (t, *J* = 7.2 Hz, 3H). ^{13}C NMR (150

MHz, $CDCl_3$) δ 164.4, 160.8, 157.0, 155.2, 142.8, 134.1, 132.5, 128.9, 127.7, 61.6, 42.0, 14.0. MS (ESI) *m/z* 337 $(M+H)^+$.

b)

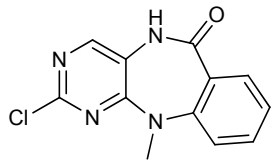

3

A mixture of compound **2** (2.35 g, 6.98 mmol) and iron power (3.9 g, 69.8 mmol) in acetic acid (100 mL) was heated at 50 ˚C for 9 hours. After the reaction was complete as monitored by reverse phase analytical liquid-chromatography electrospray mass spectrometry (LC-MS), the excess of iron was removed and the mixture was concentrated *in vacuo*. The resulting residue was poured into ice-water which resulted in a solid precipitate that was collected by filtration, washed with water and air dried to give the title compound **3** (1.55 g, 85%). ^{1}H NMR (600 MHz, DMSO-d_6) δ 10.44 (s, 1H), 8.14 (s, 1H), 7.72 (d, *J* = 4.8 Hz, 1H), 7.58 (s, 1H), 7.27 (d, *J* = 6.0 Hz, 1H), 7.21 (s, 1H), 3.33 (s, 3H). ^{13}C NMR (150 MHz, DMSO-d_6) δ 167.6, 161.4, 153.4, 149.7, 147.9, 134.2, 132.0, 125.9, 124.6, 124.3, 120.1, 37.2. MS (ESI) *m/z* 261 $(M+H)^+$.

c)

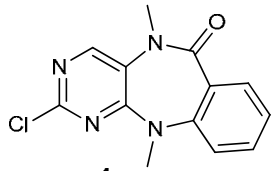

4

To a stirred suspension of compound **3** (688 mg, 2.64 mmol) and MeI (0.25 mL, 4.0 mmol) in dimethyl acetamide (DMA, 40.0 mL) was added NaH (360 mg, 60 % suspension in mineral oil) at -10 ˚C and the reaction was gradually warmed to 0 ˚C. After the reaction was complete as monitored by LC-MS, the solution was poured into ice-water which resulted in a solid precipitate. The precipitate was collected by filtration, washed with water and air dried to give the title compound

4 (563 mg, 77%). ^{1}H NMR (600 MHz, DMSO-d_6) δ 8.57 (s, 1H), 7.68 (dd, *J* = 1.2, 7.2 Hz, 1H), 7.54-7.51 (m, 1H), 7.25 (d, *J* = 7.8 Hz, 1H), 7.20-7.18 (m, 1H), 3.41 (s, 3H), 3.32 (s, 3H). ^{13}C NMR (150 MHz, DMSO-d_6) δ 167.1, 163.8, 153.7, 153.4, 148.6, 133.5, 132.4, 128.7, 126.0, 124.6, 118.9, 38.1, 36.4. MS (ESI) *m/z* 275 $(M+H)^+$.

d)

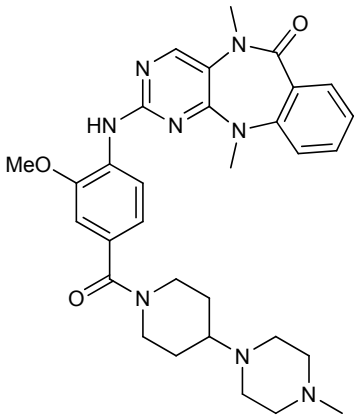

LRRK2-IN-1 (**1**)

A mixture of **4** (164.8 mg, 0.6 mmol), (4-amino-3-methoxyphenyl)(4-(4-methylpiperazin-1-yl)piperidin-1-yl)methanone **5** (199.4 mg, 0.6 mmol), 2-dicyclohexylphosphino-2′,4′,6′-tri-isopropylbiphenyl (X-Phos) (38.7 mg), tris(dibenzylideneacetone)dipalladium ($Pd_2(dba)_3$) (49.5 mg) and K_2CO_3 (331.7 mg, 2.4 mmol) in *t*-BuOH (6.0 mL) was heated at 100 ˚C for 4 hours. Then the reaction was filtered through celite and eluted with dichloromethane. The dichloromethane was removed *in vacuo* and the resulting crude product was purified by silica-gel column chromatography with ammonia solution 3.5 N in methanol and dichloromethane (1/30, v/v) to give the title compound LRRK2-IN-1 (**1**) (153.9 mg, 45%). ^{1}H NMR (600 MHz, $CDCl_3$) δ 8.48 (d, *J* = 7.8 Hz, 1H), 8.16 (s, 1H), 7.84 (dd, *J* = 1.8, 7.8 Hz, 1H), 7.76 (s, 1H), 7.44-7.41 (m, 1H), 7.13 (t, *J* = 7.8 Hz, 1H), 7.08 (d, *J* = 9.0 Hz, 1H), 7.03-7.00 (m, 2H), 3.92 (s, 3H), 3.50 (s, 3H), 3.42 (s, 3H), 3.10-2.30 (m, 13H), 2.28 (s, 3H), 2.00-1.80 (m, 2H), 1.58-1.40 (m, 2H). ^{13}C NMR (150 MHz, $CDCl_3$) δ 170.2, 168.2, 163.7, 155.4, 151.2, 149.2, 147.4, 132.4, 132.3, 130.7, 128.6, 126.4, 123.8, 121.8, 119.9, 117.4, 116.6,

109.4, 61.7, 55.9, 55.3, 49.0, 45.9, 38.2, 35.9. MS (ESI) *m/z* 571 $(M+H)^+$. HRMS (ESI) calcd for $C_{31}H_{38}N_8O_3$ 570.3067, found 571.3145 $(M+H)^+$.

Scheme 2

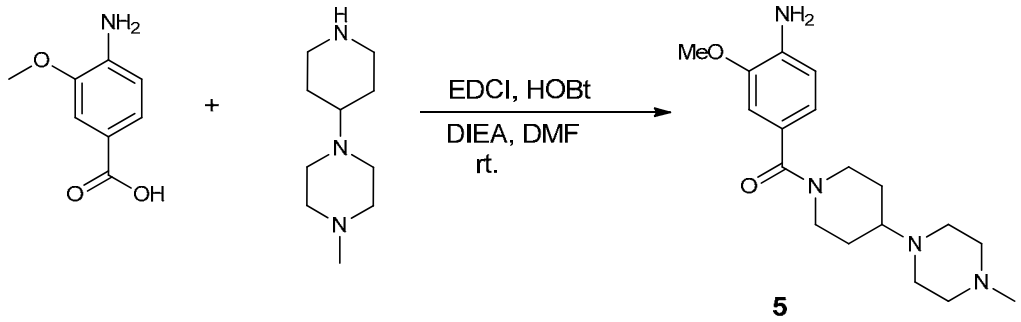

5

To a stirred solution of 4-amino-3-methoxybenzoic acid (2.0 g, 12.0 mmol), 1-methyl-4-(piperidin-4-yl)piperazine (2.2 g, 12.0 mmol), *N,N*-diisopropylethylamine (4.18 mL, 24.0 mmol) and 1-hydroxybenzotriazole (2.43 g, 18.0 mmol) in 50 mL of dimethylformamide was added 1-ethyl-3-(3-dimethylaminopropyl)carbodiimide (4.14 g, 21.6 mmol) at 0 °C. The reaction mixture was warmed up to room temperature gradually. After the reaction was complete, as monitored by LC-MS, the mixture was poured into ice-water and extracted with ethyl acetate. The organic layer was washed with brine and dried over anhydrous sodium sulfate. Then the solvent was removed in vacuo and the resulting crude product was purified by silica-gel column chromatography with ammonia solution 3.5 N in methanol and dichloromethane (1/30, v/v) to give the title compound **5** (3.39 g, 85%). ^{1}H NMR (600 MHz, $CDCl_3$) δ 6.91 (d, *J* = 1.2 Hz, 1H), 6.84 (dd, *J* = 1.8, 7.8 Hz, 1H), 6.64 (d, *J* = 7.8 Hz, 1H), 3.97 (s, 2H), 3.85 (s, 3H), 2.87-2.42 (m, 13H), 2.28 (s, 3H), 1.89-1.86 (m, 2H), 1.55-1.42 (m, 2H). ^{13}C NMR (150 MHz, $CDCl_3$) δ 170.8, 146.7, 138.0, 125.3, 120.6, 113.4, 110.1, 61.8, 55.5, 55.3, 49.1, 45.9. MS (ESI) *m/z* 333 $(M+H)^+$.

2. Biological materials and methods

Reagents and General methods. Tissue-culture reagents were from Life Technologies. P81 phosphocellulose paper was from Whatman and [γ-^{32}P]-ATP was from Perkin Elmer. Nictide and LRRKtide were synthesised by Pepceuticals. Protein G sepharose was from Amersham. Anti-GFP antibody, GFP binder Sepharose beads and myelin basic protein were provided by the Division of Signal Transduction Therapy, University of Dundee. Flag M2 agarose was from Sigma. DNA constructs used for transfection were purified from Escherichia coli DH5α using Qiagen or Invitrogen plasmid Maxi kits according to the manufacturer's protocol. All DNA constructs were verified by DNA sequencing, which was performed by The Sequencing Service, School of Life Sciences, University of Dundee, Scotland, U.K., using DYEnamic ET terminator chemistry (Amersham Biosciences) on Applied Biosystems automated DNA sequencers.

Cell culture, treatments and cell lysis. HEK-293 and Swiss 3T3 cells were cultured in Dulbecco's Modified Eagle's medium supplemented with 10% FBS, 2mM glutamine and 1X pen/strep solution. The Flp-in T-REx system was from Invitrogen and stable cell lines, generated as per manufacturer instructions by selection with hygromycin, have been described previously[1,2]. HEK-293 T-REx cell lines were cultured in DMEM supplemented with 10% FBS and 2mM glutamine, 1X pen/strep, 15 μg/ml blastocidin and 100 μg/ml hygromycin. T-Rex cultures were induced to express the indicated protein by inclusion of 0.1 μg/ml doxycycline in the culture medium for 24-48 hours. Epstein-Barr virus immortalized primary human lymphoblastoid cells from one control subject and one Parkinson's disease patient homozygous for the LRRK2 [G2019S] mutation were kindly provided by Alastair Reith (GSK) and have been described previously[3]. SHSY5Y cells were seeded into 150 cm^2 dishes at a density of 5 x 10^6 and grown to a total count of 2 x 10^7 in media consisting of 45% DMEM, 45% HAMS F12 and 10% FBS. For inhibitor experiments, LRRK2-IN-1 was dissolved in DMSO and utilised at the indicated concentrations. The concentration of

DMSO in the culture media did not exceed 1%. Following treatment, cells were washed once with PBS and lysed with buffer containing 50 mM Tris/HCl, pH 7.5, 1 mM EGTA, 1 mM EDTA, 1 mM sodium orthovanadate, 10 mM sodium β-glycerophosphate, 50 mM NaF, 5 mM sodium pyrophosphate, 0.27 M sucrose, 1 mM benzamidine, 2 mM phenylmethanesulphonylfluoride (PMSF) and 1% Triton X-100. Protein concentrations were determined following centrifugation of the lysate at 16,000 x g at 4 °C for 20 minutes using the Bradford method with BSA as the standard. Transient transfection of HEK 293 cells was performed using the PEI method [4].

IC50 determination. Active GST-LRRK2 (1326-2527), GST-LRRK2 [G2019S] (1326-2527), GST-LRRK2 [A2016T] (1326-2527) and GST-LRRK2 [A2016T+G2019S] (1326-2527) enzyme was purified with glutathione sepharose from HEK293 cell lysate 36 h following transient transfection of the appropriate cDNA constructs as described previously [5]. Peptide kinase assays, performed in duplicate, were set up in a total volume of 40 μl containing 0.5 μg LRRK2 kinase (which at approximately 10% purity gives a final concentration of 8 nM) in 50 mM Tris/HCl, pH 7.5, 0.1 mM EGTA, 10 mM $MgCl_2$, 20 μM Nictide, 0.1 μM [γ-^{32}P]ATP (~500 cpm/pmol) and the indicated concentrations of inhibitor dissolved in DMSO. After incubation for 15 min at 30 °C, reactions were terminated by spotting 35 μl of the reaction mix onto P81 phosphocellulose paper and immersion in 50 mM phosphoric acid. Samples were washed extensively and the incorporation of [γ-^{32}P]ATP into Nictide was quantified by Cerenkov counting. IC50 values were calculated with GraphPad Prism using non-linear regression analysis.

Assay of LRRK2 and LRRK1 kinase activity. Full length LRRK2 or LRRK1 was immunoprecipitated from 1 mg transiently transfected HEK293 cell lysate with 5 μl anti-FLAG agarose. Kinase assays were performed in 50 μl kinase assay buffer containing 50 mM Tris/HCl, pH 7.5, 0.1 mM EGTA, 10 mM $MgCl_2$, 0.1 μM [γ-^{32}P]ATP (~500 cpm/pmol) with either 20 μM Nictide, 100 μM LRRKtide or 2 μg

myelin basic protein as substrate. After incubation for 20 min at 30 °C, reactions were terminated by spotting 40 μl of the reaction mix onto P81 phosphocellulose paper and immersion in 50 mM phosphoric acid. Samples were washed extensively and the incorporation of [γ-^{32}P]ATP into substrate was quantified by Cerenkov counting. Autophosphorylation of LRRK1 and LRRK2 and phosphorylation of a denatured fragment of moesin encompassing residues 400-552 (prepared as in [5]) were assessed following incubation in the same kinase buffer described above. Reactions were terminated with the addition of 4 x LDS sample buffer (Invitrogen) and proteins separated on a 4-12% gradient gel (Invitrogen) before colloidal blue staining and autoradiograph. The final concentration of moesin 400-552 in the reaction was 2 μM.

Immunoprecipitation and immunoblot procedures. Endogenous LRRK2 was immunoprecipitated from 9 mg protein lysate from Swiss 3T3 cells and human lymphoblastoid cells or 10 mg protein lysate from SHSY5Y cells using 15 μg of our previously characterised LRRK2 100-500 antibody[1] coupled to 30 μl of Protein G-Sepharose. Cell lysates were incubated with antibody-coupled beads for 1-2 hours. Immune complexes were then washed twice with lysis buffer supplemented with 0.5 M NaCl and twice with Buffer A (50 mM Tris/HCl, pH 7. 0.1 mM EGTA). Immunoprecipitates were then eluted in 65 μl 2x LDS sample buffer (Invitorgen) and separated from the Sepharose beads using 0.2 μm Spinex columns. Following heating at 70°C for 10 min 15 μL aliquots were resolved on 8% SDS polyacrylamide gels and transferred to nitrocellulose membranes for detection of LRRK2 phosphorylated at S910, LRRK2 phosphorylated at S935, total LRRK2 and 14-3-3 binding. Membranes were blocked for 1h with 5% skimmed milk (w/v) in 50 mM Tris/HCl, pH 7.5, 0.15 M NaCl and 0.1% (v/v) Tween (TBST). Previously characterised phospho-specific antibodies for the detection of LRRK2 S910 and S935 phosphorylation were used at a concentration of 1 μg/ml in blocking buffer overnight with the inclusion of 10 μg/ml dephosphorylated peptide[2]. Detection of immune-complexes was performed using a fluorophore conjugated rabbit anti-sheep secondary antibody

(Molecular Probes) followed by visualisation and quantitation using an Odyssey LICOR. Digoxigenen (DIG) labelled 14-3-3 for use in overlay far western analysis was prepared as described in [6]. Membranes were incubated with DIG labelled 14-3-3 diluted to 0.5 µg/ml in 5% BSA in TBST overnight at 4 ^{o}C. DIG 14-3-3 was detected with HRP labelled anti-DIG Fab fragments (Roche). For GFP-LRRK2 expressing stable cell lines, 20 µg protein lysate was resolved on 8% polyacrylamide gels and immunoblotted for LRRK2 phosphorylated at S910 and LRRK2 phosphorylated at S935 as above. Total levels of GFP tagged LRRK2 were assessed using a sheep anti-GFP antibody. In some instances phosphorylated S910 immunoblots were stripped with 1x re-blot plus (Millipore) before reprobing with anti-GFP. 14-3-3 binding in these cell lines was determined by 14-3-3 overlay, as above, following immunoprecipitation from 0.5 mg protein lysate with 5 µl GFP –binder Sepharose. Original images for all immunoblots cropped for presentation in supplementary figures are available to view in supplementary figure 12.

Fluorescence Microscopy. HEK-293 Flp-in T-REx cells harbouring GFP tagged LRRK2 or LRRK1 were grown on 18 mm x 18 mm glass coverslips (VWR international) pre treated with 50 µg/ml Poly-Lysine (Chemicon). One day after plating, cells were induced with 0.1 µg/ml doxycycline for 24 hr. Cells were then treated with inhibitor or DMSO as indicated. Media was removed at the completion of the experiment and cells were washed twice with PBS before being fixed in 4% paraformaldehyde buffered in phosphate buffered saline (USB). Fixed cells were again washed with PBS and then mounted in ProLong Gold (Invitrogen) and imaged on a Zeiss LSM 700 confocal microscope using an α Plan-Apochromat x100 objective. For live cell imaging experiments GFP-LRRK2 expressing cells were plated into 17 mm glass bottom Willco-dishes (Intracell). One day after plating LRRK2 expression was induced with 0.1 µg/ml doxycycline for 24 hr. Cells were filmed for 15 min and then for a further 90 min following addition of 1 µM LRRK2-IN-1. For washout fixed slides and movies, inhibitor-containing media was removed and cells were washed twice with fresh media

before fixing or the recommencement of filming. Time-lapse movies were recorded using the α Plan-Apochromat x100 objective, one frame was recorded every 30 seconds. The cells were maintained at 37 ^{o}C and 5% CO_2 using a stage incubator and heated stage plate (Incubator S and insert P, Carl Zeiss). The percentage of GFP-LRRK2 [G2019S] or GFP-LRRK2 [A201TS+G2019S] cells expressing aggregates was determined following treatment of cells with 1 μM LRRK2-IN-1 for 2 h before fixing cells as above. Fixed cells were then counter stained with DAPI (Sigma) before fluorescence imaging. Thirty images for each cell line were obtained at random and the number of cells expressing more than three aggregate or fibrilar structures per cell were counted and divided by the total number of nuclei in each field.

Injection into mice.

LRRK2-IN-1 was dissolved in Captisol (Cydex Pharmaceuticals) and administered by intraperitoneal injection into wild type male C57BL/6 mice at a dose of 100 mg/kg. Control mice were injected with an equal volume of Captisol. At 1 and 2 h time points, mice were extinguished by cervical dislocation and kidney and brain tissue rapidly dissected and snap-frozen in liquid nitrogen. Animal experiments were approved by the University of Dundee Ethics Committee and performed under a U.K. Home office project license.

Statistical analysis.

GraphPad Prism was used to analyse quantitated immunoblots by one-way ANOVA. Significance between groups was determined using Tukey's post hoc test with significance accepted at $p < 0.05$.

Supplementary results

LRRK2-IN-1 selectivity profiling

The kinase selectivity of LRRK2-IN-1 was evaluated using the KINOME*scan*™ methodology (Ambit Biosciences, San Diego, CA)[7,8], the KiNativ™ technology (ActivX Biosciences, San Diego, CA)[9], and standard radioactive-based enzymatic assays (Dundee profiling)[10] (Result details see **Supplementary Dataset**) .

The selectivity score (S (3 μM)) for LRRK2-IN-1 calculated by dividing the number of kinases found to bind with a dissociation constant (K_d < 3 μM) by the total number of kinases tested is 0.029 (13/442), which represents high selectivity. For reference, the highly selective Her2 inhibitor lapatinib has an (S (3 μM)) of 0.038 (12/317) while an inhibitor like imatinib has an (S (3 μM)) of 0.082 (26/317)[8].

PLK1 cellular activity of LRRK2-IN-1

For PLK1 we observed a 100-fold discrepancy between the observed ambit *K*d (75 nM) and the biochemical enzyme assay (IC_{50} = 9.83 uM from invitrogen, IC_{50} > 100 uM from Dundee) and further cellular experiments (described below) demonstrated that LRRK2-IN-1 is not a potent PLK1 inhibitor.

To establish whether LRRK-IN-1 can inhibit PLK1 in cells we took advantage of the observation made using both RNAi and inhibitors that loss of PLK1 function results in a prometaphase arrest[11,12]. LRRK2-IN-1 was added in a dilution series to HeLa S3 cells and incubated for 18 hrs. As a control, BI2536 – a highly potent PLK1,2,3 inhibitor was added to cells at 100 and 500 nM. Both concentrations of BI2536 produced an efficient mitotic arrest, while arrested cells were only observed for LRRK2-IN-1 at a concentration of 10 uM which is well beyond the concentrations required to inhibit cellular LRRK2 activity.

Supplementary Table 1.

The combined kinase profiling hits with biochemical activities. Kinase hits from Ambit profiling with a score of less than 10% of the DMSO control at a concentration of 10 μM, ActivX profiling with higher than 50% inhibition at 1 μM, and Dundee profiling with greater than 50% inhibition at 1 μM are listed. The biochemical IC_{50} values of hits were measured by Invitrogen Adapta®, Z´-Lyte®, Lantha-Screen® assays (http://www.invitrogen.com/site/us/en/home/Products-and-Services/Services/ Screening-and-Profiling-Services/SelectScreen-Profiling-ervice/SelectScreen-Kinase-Profiling-Service.html) and Dundee radioactive-base enzyme assay[10].

Kinase Label	% Ctrl at 10 μM (Ambit)	Binding assay K_d (μM, Ambit)	Biochemical assay IC_{50} (μM, Invitrogen)	Biochemical assay IC_{50} (μM, Dundee)
AURKA	1.2	1.60	0.87	1.20
AURKB	38	ND	5.92	1.10
CHEK2	66	ND	6.51	2.00
DCLK1	4.2	0.005	NA	NA
DCLK2	0.45	0.016	0.045	0.21
LRRK2	0	0.020	0.003	0.013
LRRK2(G2019S)	5	0.011	0.004	0.006
MAPK7	0.05	0.028	NA	NA
MKNK2	1.2	0.38	4.47	7.20
MYLK	8.7	ND	8.21	12.20
NUAK1	47	ND	3.67	5.00
PLK1*	0.7	0.075	9.83	>100
PLK4	0	0.016	NA	NA
RPS6KA2(Kin.Dom2-C-terminal)	7.5	1.00	NA	NA
RPS6KA6(Kin.Dom2-C-terminal)	2.2	0.62	NA	NA
TNK1	2.8	0.023	NA	NA

Supplementary Table 2.

Pharmacokinetic Parameters of LRRK2-IN-1 in Mice

Route	Dose (mg/kg)	T_{max} (h)	C_{max} (ng/mL)	$AUC_{0-\infty}$ (hr*ng/mL)	$T_{1/2}$ (hr)	CL (mL/min/Kg)	V_{ss} (L/Kg)	F (%)
IV	1	-	-	2974	4.47	5.6	1.71	-
PO	10	1.0	1618	14758	-	-	-	49.3

* IV = intravenous injection, PO = oral delivery, T_{max} = time of maximum plasma concentration, C_{max} = maximum plasma concentration, AUC = area under the curve (measure of exposure), $T_{1/2}$ = half life, CL = plasma clearance, Vss = volume of distribution, F = oral bioavailability.

Supplementary Fig.1 IC_{50}s of LRRK2-IN-1 against LRRK2[G2019S]
LRRK2[G2019S] (1326-2527) was assayed in the presence of different concentrations of ATP using the indicated concentrations of LRRK2-IN-1. Results are presented as percentage of kinase activity relative to the DMSO treated control. Results are averages of duplicate reactions. The IC_{50} values were derived from graphs which were generated with Graphpad Prism using non linear regression analysis.

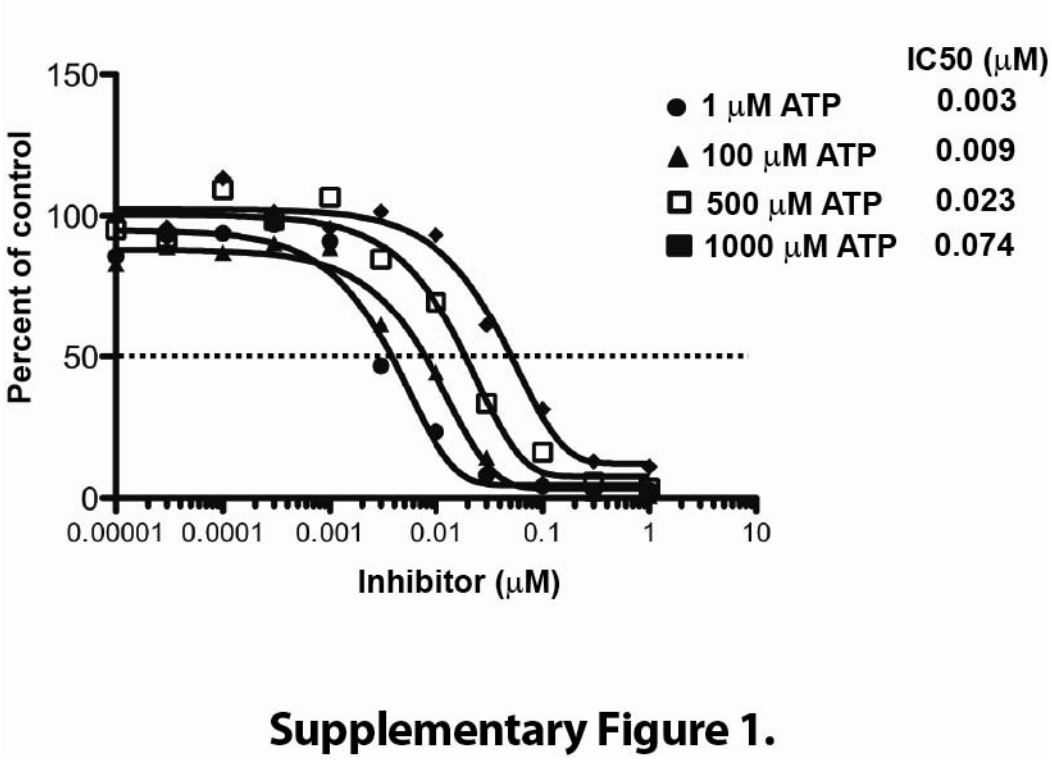

Supplementary Figure 1.

Supplementary Fig. 2 Molecular model of LRRK2-IN-1 bound to a homology model of LRRK2 (colored ribbons).
LRRK2-IN-1 (green sticks) occupies the ATP binding site with two hydrogen bonds between the aminopyrimidine to the kinase hinge segment. The A2016T mutation is indicated in red.

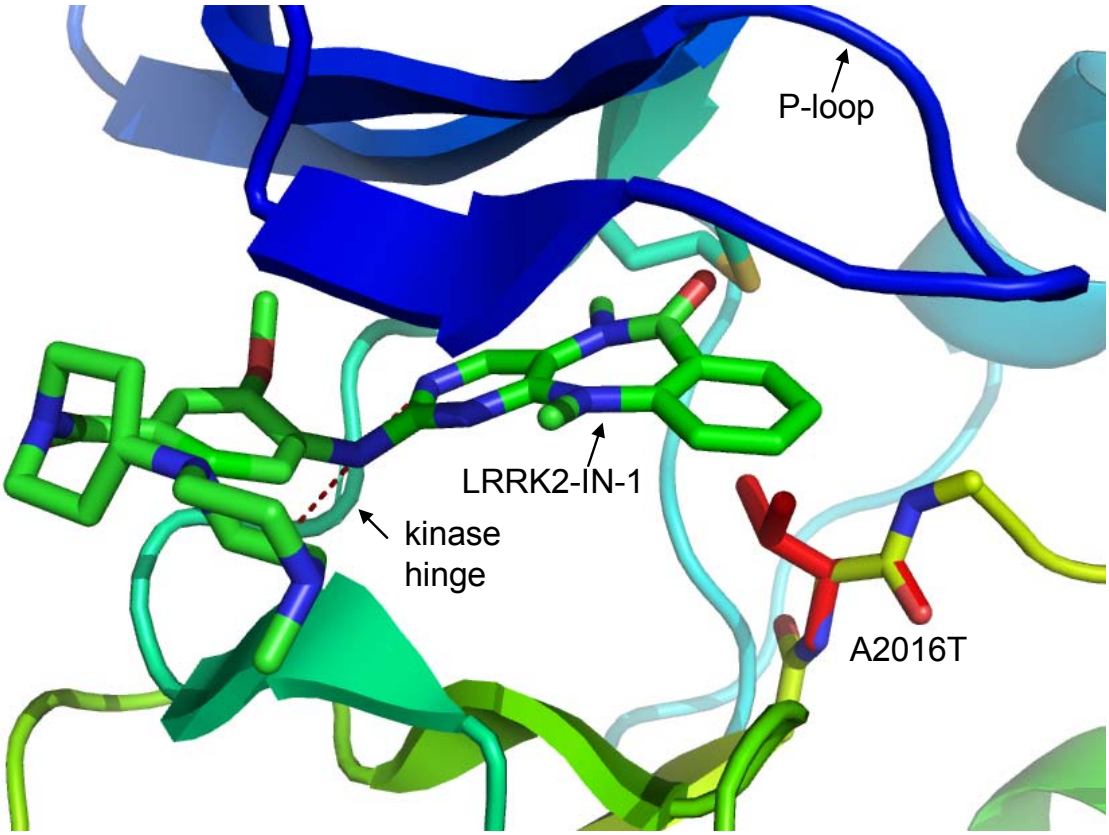

Supplementary Fig. 3 Cellular EC_{50} of LRRK2-IN-1 against MAPK7

HeLa cells were serum starved overnight followed by treatment with different concentrations of LRRK2-IN-1 for 1 hr. Cells were then stimulated with EGF for 17 min and MAPK7 activation was detected by mobility retardation[13].

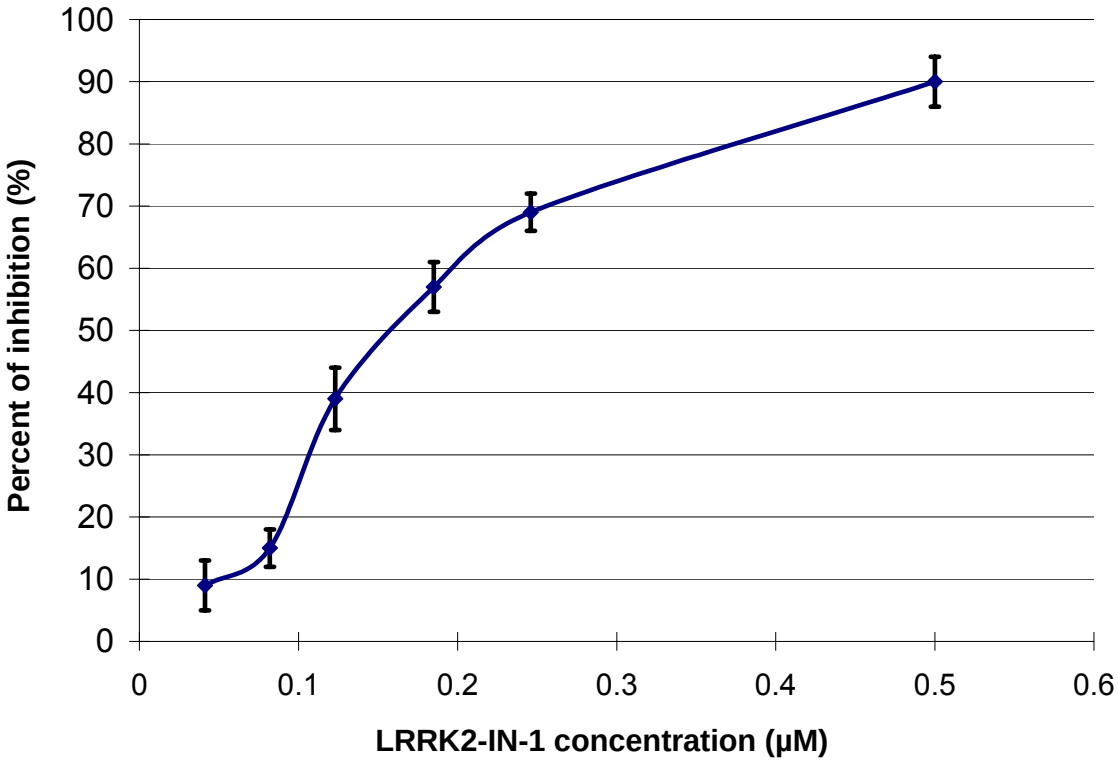

Supplementary Fig. 4 LRRK1 is inactive against LRRK2 substrates in vitro.

(**A**) Full length flag-tagged LRRK1 and LRRK2 were transfected into HEK 293 cells and expressed at similar levels. (**B**) Flag-empty and full length flag-LRRK1 and flag-LRRK2 were immunoprecipitated with anti-flag agarose from 1 mg transient transfected HEK293 cell lysate and used as a source of kinase for in vitro peptide kinase assays with either 100 μM LRRKtide, 20 μM Nictide or 2 μg myelin basic protein as substrate. Reactions were performed in duplicate and results are representative of at least three independent experiments. Data is presented as mean ± SEM. (**C**) Full length flag tagged wildtype and kinase dead LRRK1 and LRRK2 were immunoprecipitated with anti-flag agarose from 5 mg transiently transfected HEK293 cell lysate and were used to phosphorylate 2 μM of a C-terminal fragment of moesin encompassing residues 400-577.

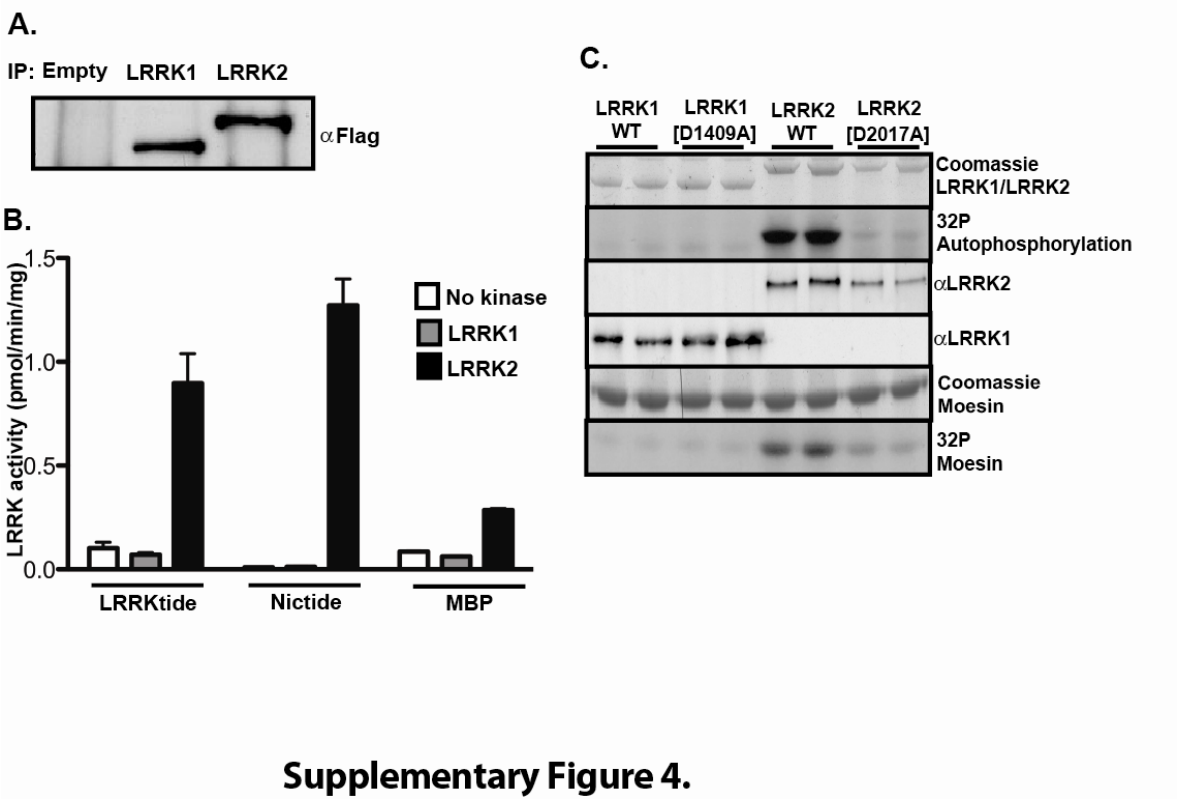

Supplementary Figure 4.

Supplementary Fig. 5 LRRK2-IN-1 is a reversible inhibitor.

(**A**) HEK 293 cells stably expressing wild type GFP-LRRK2 were treated with 1 μM LRRK2-IN-1 for the indicated time points. To determine LRRK2 re-phosphorylation, inhibitor-containing media was removed 2 h after treatment, cells were washed twice and incubated with fresh media without inhibitor for the indicated time points. Cell lysates were subjected to immunoblotting for detection of LRRK2 phosphorylated at S910 and S935 and for total GFP-LRRK2. 14-3-3 binding was measured by overlay assay following immunoprecipitation of LRRK2 with GFP-binder sepharose. (**B**) As in (**A)** except HEK 293 cells stably expressing GFP-LRRK2 [G2019S] were utilised. (**C**) as in (**A**) except HEK 293 cells stably expressing drug resistant GFP-LRRK2 [A2016T] were utilised. (**D**) as in (**A**) except HEK 293 cells stably expressing drug resistant GFP-LRRK2[A2016T+G2019S] cells were utilised. Immunoblot analysis was quantified by Odyssey LICOR with the top graph representing the ratio of LRRK2 S910 phosphorylation to total LRRK2 and the bottom graph representing the ratio of LRRK2 S935 phosphorylation to total LRRK2. Results are representative of at least two independent experiments.

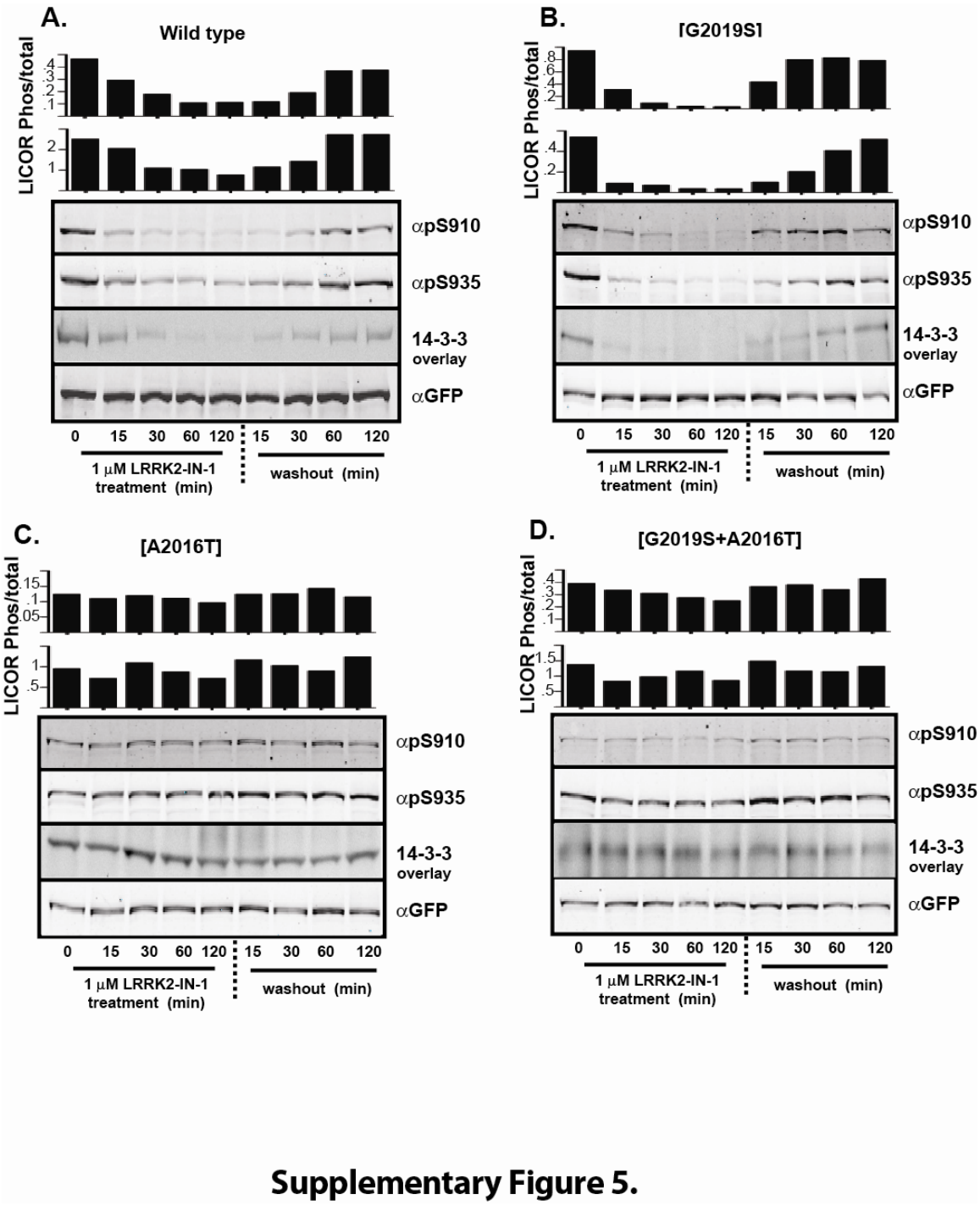

Supplementary Figure 5.

Supplementary Fig. 6 LRRK2-IN-1 does not induce dephosphorylation of kinase dead LRRK2.

Stable cell lines expressing full length flag-tagged wild type and kinase inactive LRRK2 {D2017A] were treated with 1 μM LRRK2-IN-1 for 2 h. Phosphorylation of Ser910 and Ser935 was assessed by immunoblot. 14-3-3 binding was assessed by overlay assay. Immunoblot analysis was quantified by Odyssey LICOR with the top graph representing the ratio of LRRK2 S910 phosphorylation to total LRRK2 and the bottom graph representing the ratio of LRRK2 S935 phosphorylation to total LRRK2. The experiment was performed in duplicate and results are representative of two independent experiments. Data is presented as mean ± SEM.

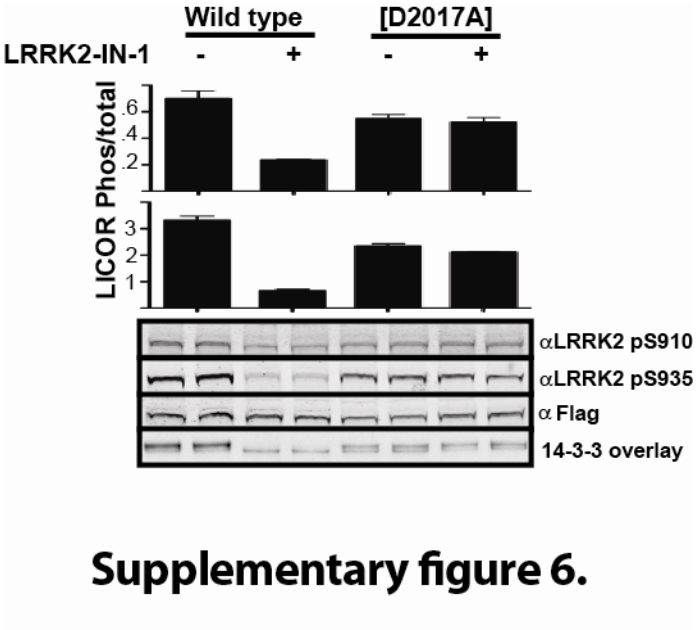

Supplementary figure 6.

Supplementary Fig. 7 Effect of LRRK2-IN-1 in Swiss 3T3 cells.
Endogenous LRRK2 was immunoprecipitated from 9 mg Swiss 3T3 cell lysate using anti-LRRK2 100-500 following treatment of cells with indicated doses of LRRK2-IN-1 for 2 h. Immunoprecipitates were subjected to immunoblot analysis and 14-3-3 overlay assay. Immunoprecipitations were performed in duplicate and results are representative of two independent experiments. Immunoblot analysis was quantified by Odyssey LICOR with the top graph representing the ratio of LRRK2 S910 phosphorylation to total LRRK2 and the bottom graph representing the ratio of LRRK2 S935 phosphorylation to total LRRK2. One-way ANOVA and Tukey's post hoc test were used to test for significant difference between LRRK2-IN-1 treatment and DMSO control. * = $p < 0.05$ compared to DMSO. Data are presented as mean ± SEM

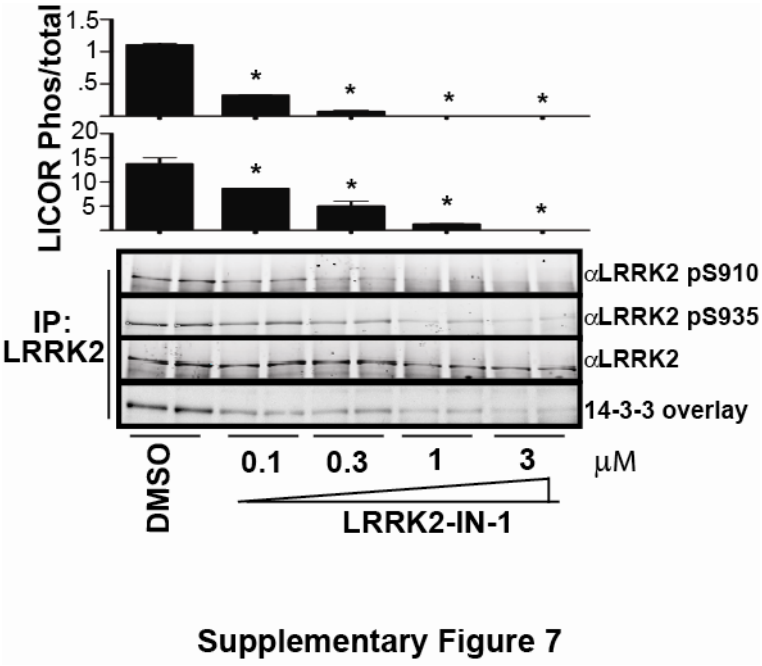

Supplementary Figure 7

Supplementary Fig. 8 LRRK2-IN-1 alters the cytoplasmic localization of LRRK2

HEK 293 cells stably expressing GFP-LRRK2 **(a)** or GFP-LRRK2 [A2016T] **(b)** or GFP-LRRK2[A2016T+G2019S] **(c)**, were treated with 1 μM LRRK2-IN-1 for indicated time points. Cells were then washed and fixed with 4% paraformaldehyde for fluorescence imaging. To visualize LRRK2 localization following removal of LRRK2-IN-1, inhibitor-containing media was removed 2 h after treatment. Cells were then washed twice and incubated with fresh media without inhibitor for the indicated time points before again being washed and then fixed for fluorescence imaging. Aggregate structures are highlighted by white arrows. Representative micrographs of three independent experiments are presented.

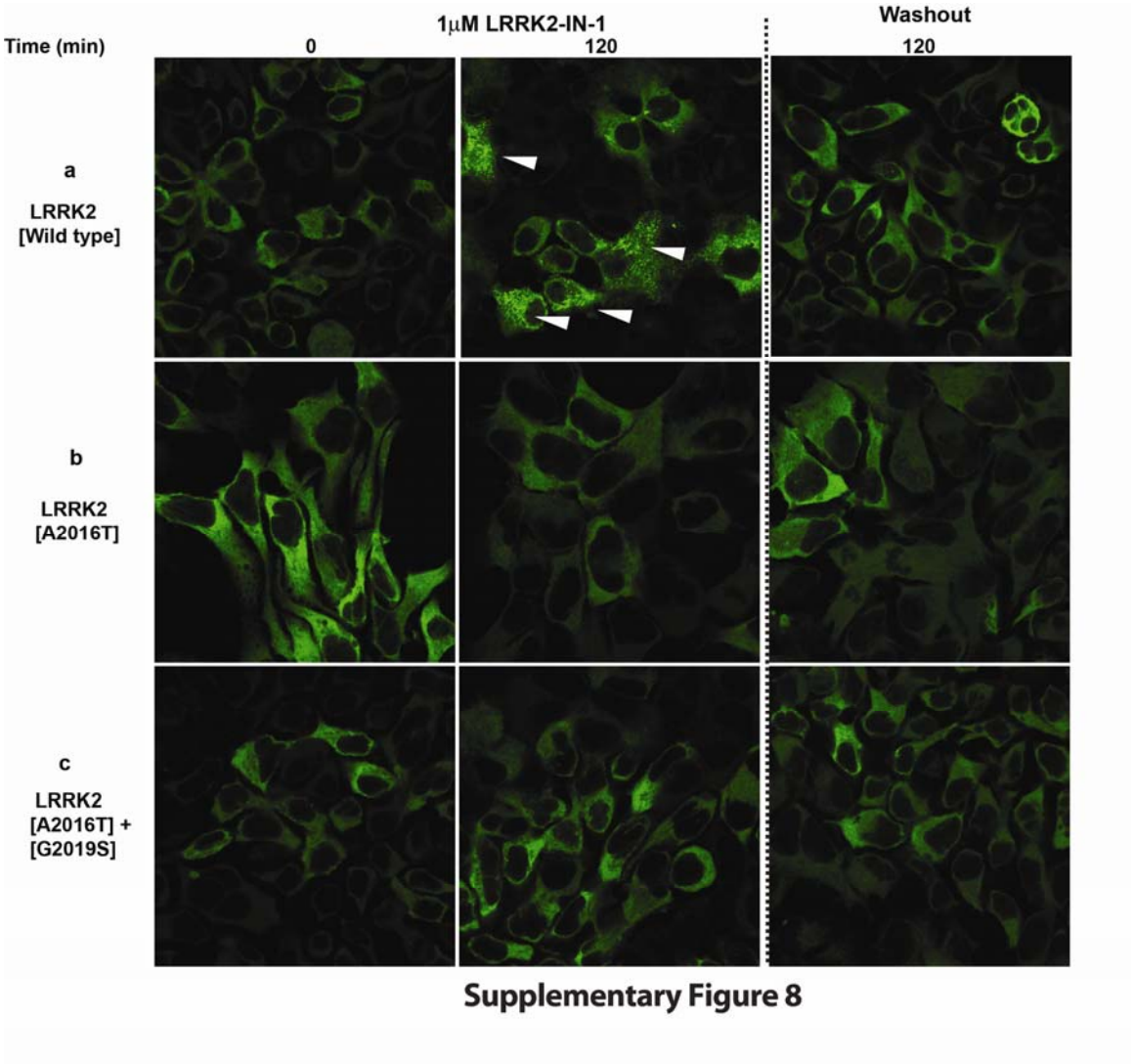

Supplementary Figure 8

Supplementary Fig. 9 The quantitation of the cell aggregates

HEK 293 cells stably expressing GFP-LRRK2 [G2019S] or GFP-LRRK2 [A2016T+G2019S] were treated with 1 μM LRRK2-IN-1 for 2 hours. Cells were then washed and fixed with 4% paraformaldehyde before counter staining with DAPI and fluoresence imaging. Cells containing greater than three aggregates or fibrilar structures per cell were quantitated from thirty images selected at random from three different experiments. The number of cells with greater than three aggregates was divided by the number of nuclei in each field to obtain the percentage of cells with aggregates. Data are presented as mean ± SEM

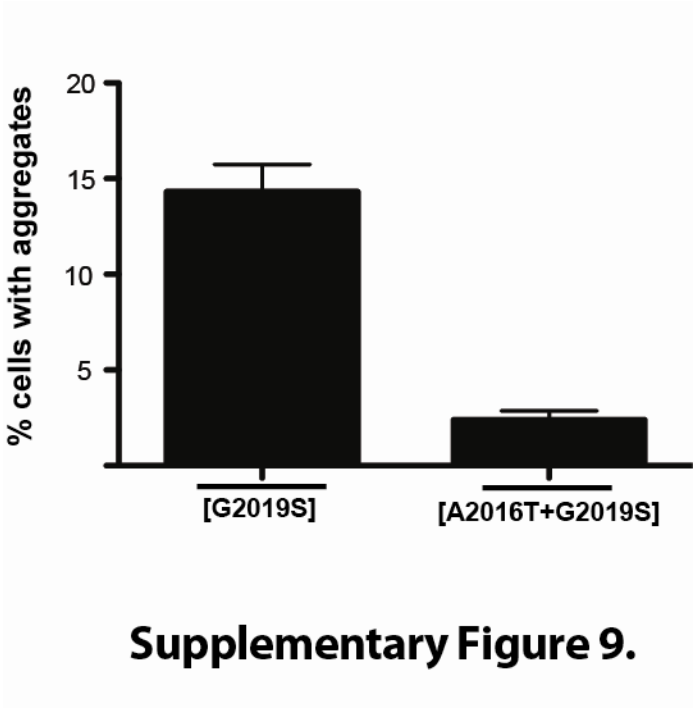

Supplementary Figure 9.

Supplementary Fig. 10 LRRK1 does not bind 14-3-3 and remains cytoplasmic

(**A**) GFP empty and full length GFP-LRRK1 and GFP-LRRK2 were immunoprecipitated from 1 mg lysate from inducible HEK 293 stable cell lines and 14-3-3 binding was assessed by overlay assay (**B**). HEK 293 cells stably expressing full length GFP-LRRK1 and GFP-LRRK2 were treated with 1 μM LRRK2-IN-1 for 2 hours. Cells were then washed and fixed with 4% paraformaldehyde for fluorescence imaging.

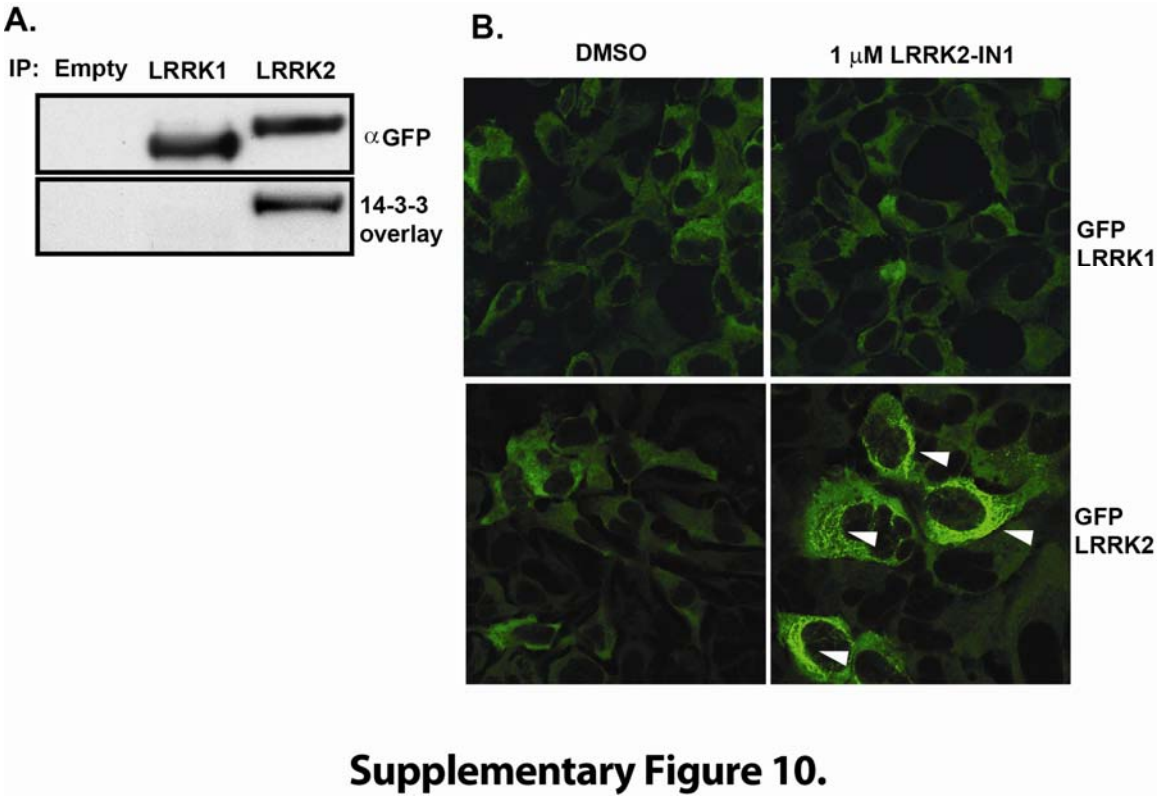

Supplementary Figure 10.

Supplementary Fig. 11 Quantitation and images for Figure 2.

Immunoblots for the detection of phosphorylated or total LRRK2 where scanned using the odyssey LICOR. Membranes were scanned from the 100kDa marker to the top (molecular weight of LRRK2 = 280 kDa). Experiments were performed in duplicate and results are representative of at least two independent experiments. Representative immunoblots were quantitated using the odyssey LICOR software. The top graph represents the ratio of LRRK2 phosphorylated at Ser910 to total LRRK2 whilst the bottom graphs represent the ratio of LRRK2 phosphorylated at Ser935 to total LRRK2. Data is presented as mean ± SEM. One-way ANOVA followed by Tukey's post hoc test was used to test for significant differences between LRRK2-IN-1 treated groups and DMSO control with * representing $p < 0.05$ compared to DMSO. 14-3-3 binding was assessed by overlay assay followed by detection with enhanced chemiluminescence. For the overlay assay membranes were again cut at the 100kDa marker.

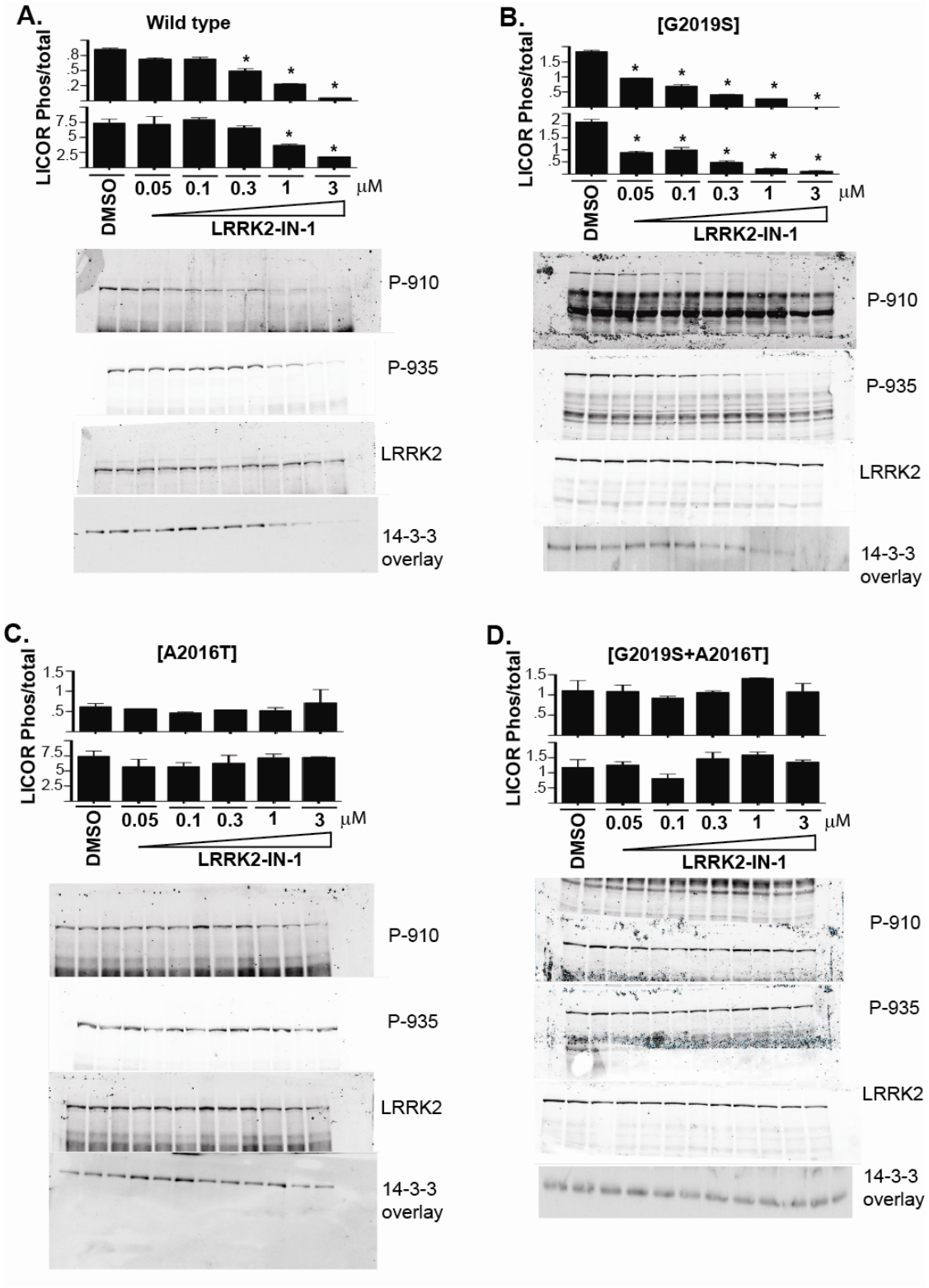
A.
Wild type
LICOR Phos/total
.8
.5
.2
7.5
5
2.5
DMSO
0.05
0.1
0.3
1
3
μM
LRRK2-IN-1
P-910
P-935
LRRK2
14-3-3
overlay
B.
[G2019S]
LICOR Phos/total
1.5
1
.5
2
1.5
1
.5
DMSO
0.05
0.1
0.3
1
3
μM
LRRK2-IN-1
P-910
P-935
LRRK2
14-3-3
overlay
C.
[A2016T]
LICOR Phos/total
1.5
1
.5
7.5
5
2.5
DMSO
0.05
0.1
0.3
1
3
μM
LRRK2-IN-1
P-910
P-935
LRRK2
14-3-3
overlay
D.
[G2019S+A2016T]
LICOR Phos/total
1.5
1
.5
1.5
1
.5
DMSO
0.05
0.1
0.3
1
3
μM
LRRK2-IN-1
P-910
P-935
LRRK2
14-3-3
overlay

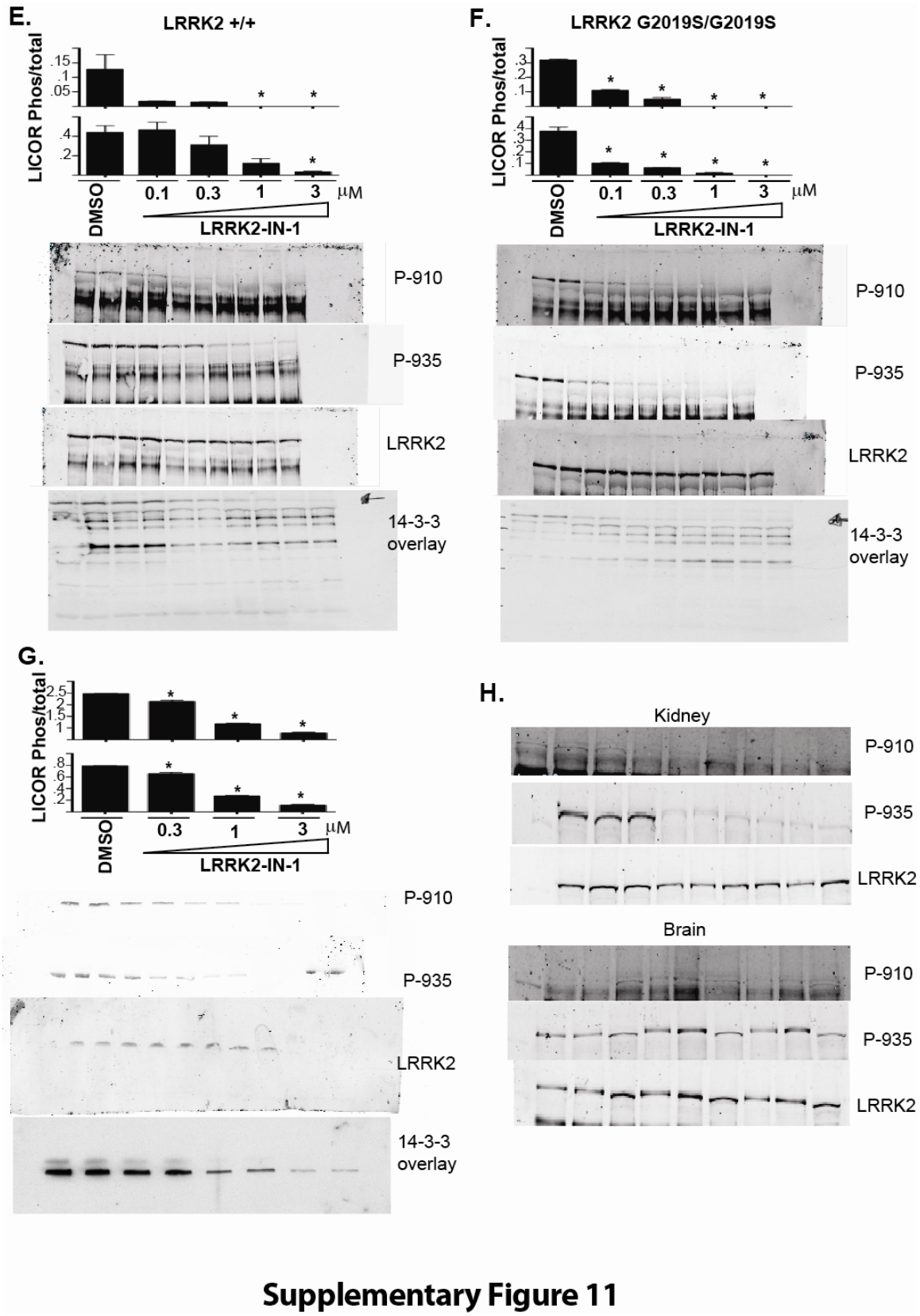

Supplementary Figure 11

Supp Figure 4a
Flag

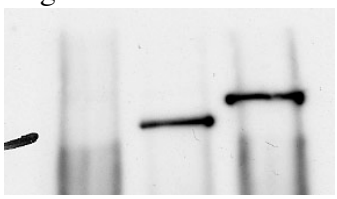

Supp Figure 4c
LRRK1

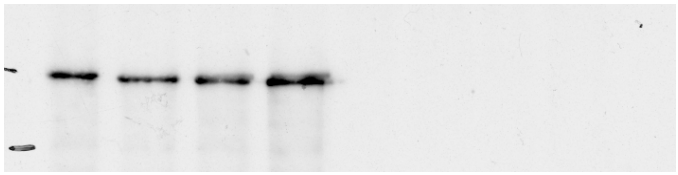

LRRK2

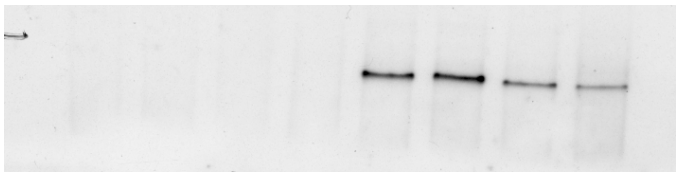

Coomassie stain

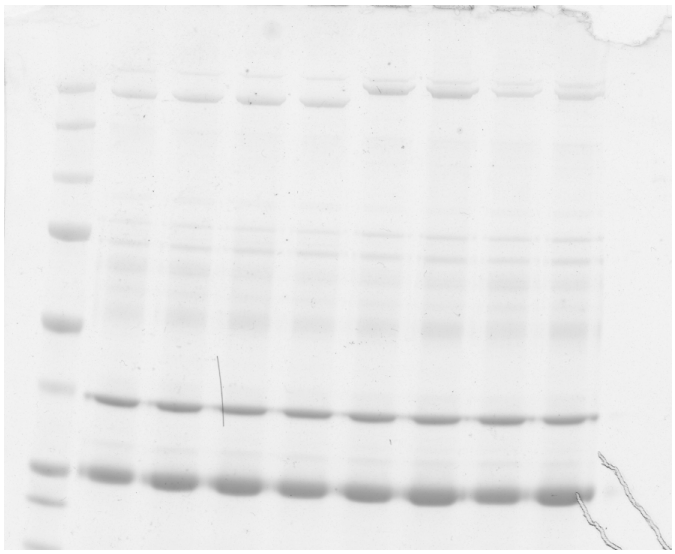

Autorad

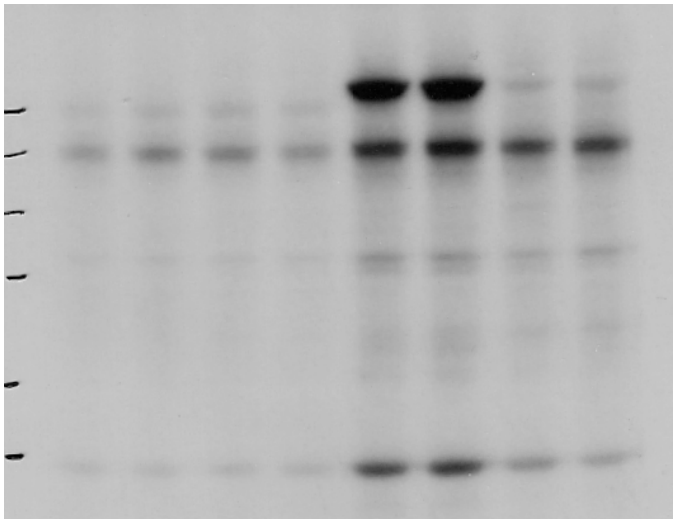

Supp Figure 5a
Phospho serine 910

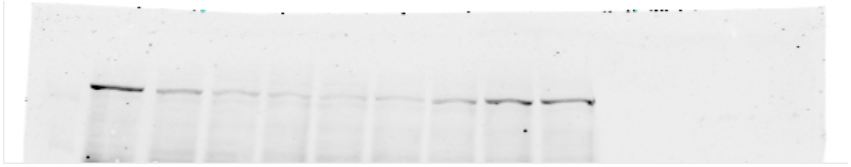

Phospho serine 935

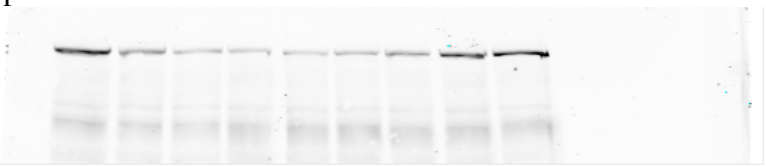

GFP

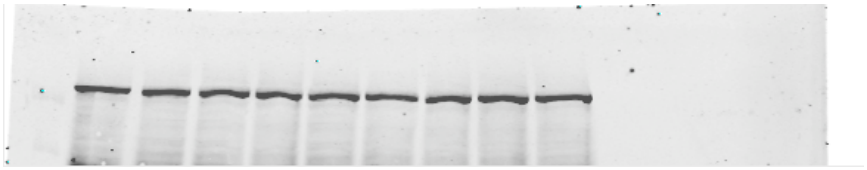

14-3-3 overlay

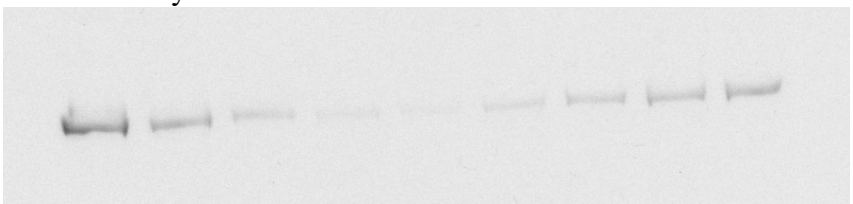

Supp Figure 5b
Phospho serine 910

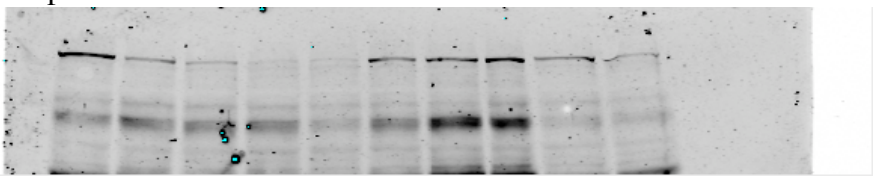

Phospho serine 935

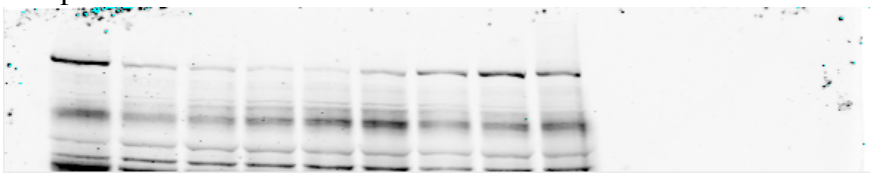

GFP

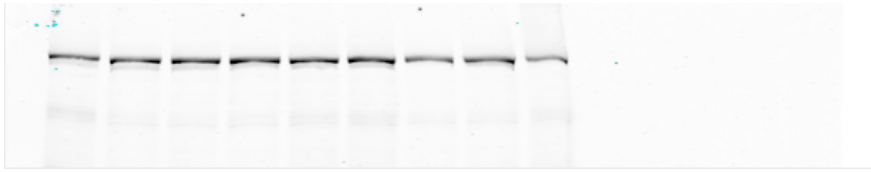

14-3-3 overlay

Supp Figure 5c

Phospho serine 910

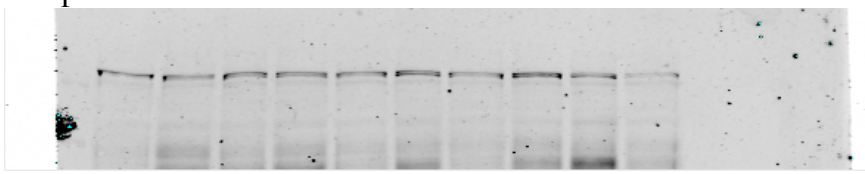

Phospho serine 935

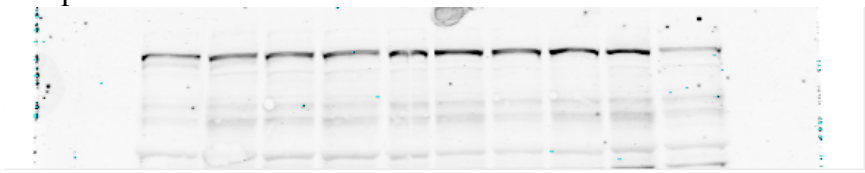

GFP

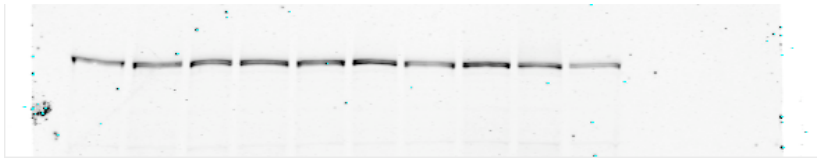

14-3-3 overlay

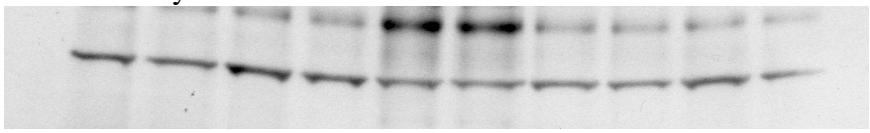

Supp Figure 5d

Phospho serine 910

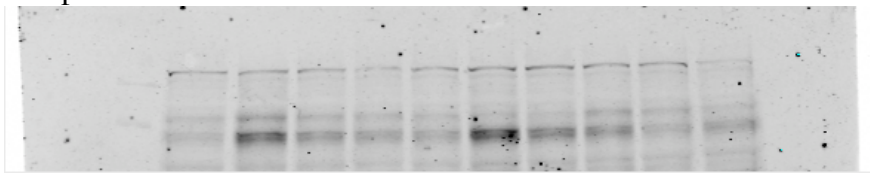

Phospho serine 935

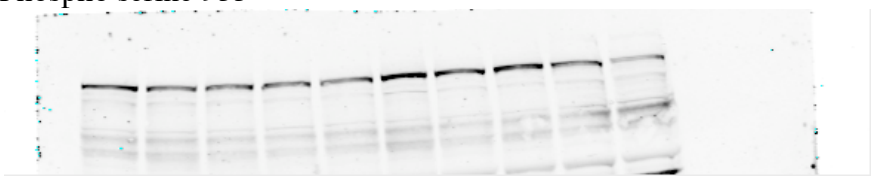

GFP

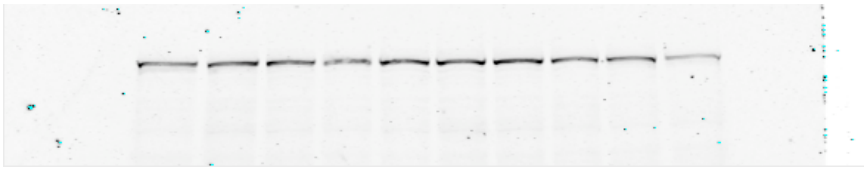

14-3-3 overlay

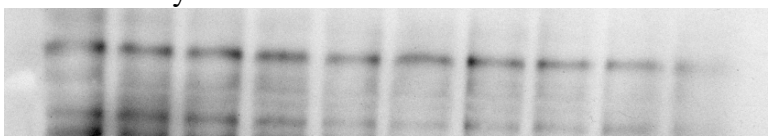

Supp Figure 6
Phospho Serine 910

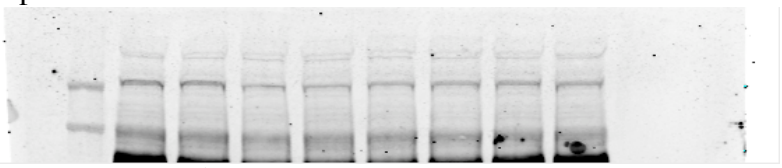

Phospho serine 935

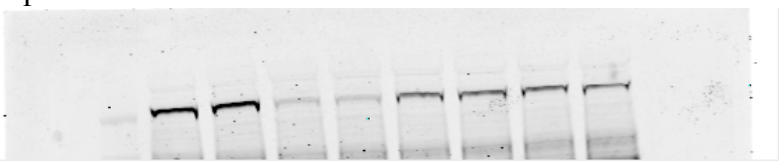

Flag

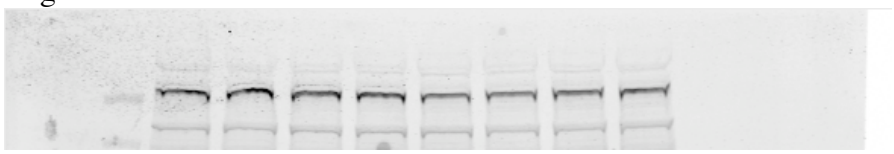

14-3-3 overlay

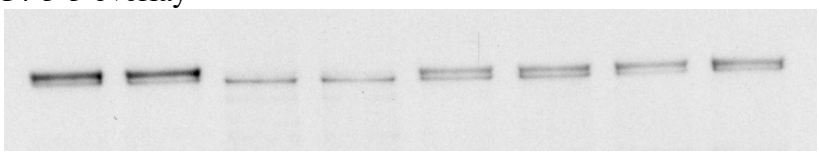

Supp Figure 7
Phospho serine 910

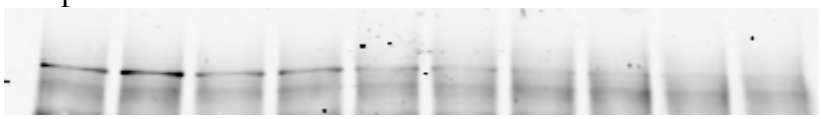

Phospho serine 935

total LRRK2

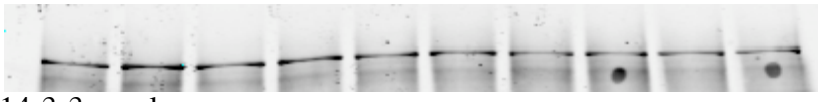

14-3-3 overlay

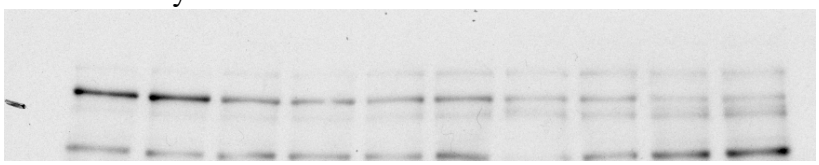

Supp Figure 10a
GFP

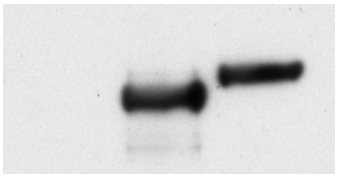

14-3-3 overlay

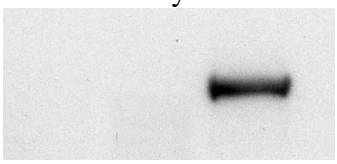

References

1. Nichols, R.J. et al. Substrate specificity and inhibitors of LRRK2, a protein kinase mutated in Parkinson's disease. *Biochem. J.* **424**, 47-60 (2009).
2. Nichols, J. et al. 14-3-3 binding to LRRK2 is disrupted by multiple Parkinson's disease associated mutations and regulates cytoplasmic localisation. *Biochem. J.* **430**, 393-404 (2010).
3. Dzamko, N. et al. Inhibition of LRRK2 kinase activity leads to dephosphorylation of Ser910/Ser935, disruption of 14-3-3 binding and altered cytoplasmic localisation. *Biochem. J.* **430**, 405-413 (2010).
4. Durocher, Y. et al., High level and high-throughput recombinant protein production by transient transfection of suspension-growing human 293-EBNA1 cells. *Nucleic Acids Res*. **30**, E9 (2002).
5. Jaleel, M. et al. LRRK2 phosphorylates moesin at threonine-558: characterization of how Parkinson's disease mutants affect kinase activity. *Biochem. J.* **405**, 307-17 (2007).
6. Moorhead, G. et al. Phosphorylation-dependent interactions between enzymes of plant metabolism and 14-3-3 proteins. *Plant J.* **18**, 1-12 (1999).
7. Fabian, M.A. et al. A small molecule-kinase interaction map for clinical kinase inhibitors. *Nat. Biotechnol.* **23**, 329-36 (2005).
8. Karaman, M.W. et al. A quantitative analysis of kinase inhibitor selectivity. *Nat. Biotechnol.* **26**, 127-32 (2008).
9. Patricelli, M.P. et al. Functional interrogation of the kinome using nucleotide acyl phosphates. *Biochemistry* **46**, 350-8 (2007).
10. Bain, J. et al. The selectivity of protein kinase inhibitors: a further update. *Biochem. J.* **408**, 297-315 (2007).
11. Lenart, P. et al. The small-molecule inhibitor BI 2536 reveals novel insights into mitotic roles of polo-like kinase 1. *Curr. Biol.* **17**, 304-15 (2007).
12. Steegmaier, M. et al. BI 2536, a potent and selective inhibitor of polo-like kinase 1, inhibits tumor growth in vivo. *Curr. Biol.* **17***,* 304-15 (2007).

13. Abe, J., Kusuhara, M., Ulevitch, R.J., Berk, B.C. & Lee, J.D. Big mitogen-activated protein kinase 1 (BMK1) is a redox-sensitive kinase. *J. Biol. Chem.* **271**, 16586-90 (1996).